ANALYSIS OF THE SUPERSONIC FLOW OF A VISCOUS HEAT-CONDUCTING GAS IN THE NEIGHBORHOOD OF A BACKWARD STEP

A. N. Antonov, A. E. Duisekulov, and T. G. Elizarova

UDC 519.6:533.6

Results are presented of numerical modelling of the supersonic flow of a viscous heat conducting gas in the neighborhood of a backward step for the Mach number $M_\infty = 2.9$ and the Reynolds number $Re_\infty = 9.5 \cdot 10^3 - 3.2 \cdot 10^4$. Kinetically consistent difference schemes are used to perform the computations. The results obtained are compared with the data of full-scale experiments.

INTRODUCTION

One of the urgent problems of modern aerodynamics is the modelling of supersonic viscous separation flows of both stationary and nonstationary type. Of special interest in such computations is the determination of the thermal loads on the specimen walls, for whose computation dissipative properties of the gas at the solid walls must be taken into account. According to modern representations, these phenomena can be described within the framework of the Navier–Stokes equations without application of additional a priori information. However, utilization of methods relying directly on the Navier–Stokes equations is fraught with considerable calculational complexities. The kinetically consistent difference schemes (KCDS) applied in this paper permit the construction of numerical solutions for such problems in the flow domain as a whole.

The KCDS [1-3] differ from other algorithms for the solution of the gas dynamics equations as follows. A difference scheme is first written down for the Boltzmann equation, which is then averaged by using the concept of a locally Maxwell or Navier–Stokes kind of distribution function, for the construction of the KCDS. To a significant extent this procedure is analogous to that used to obtain the Euler or Navier–Stokes equations from the transport equations. These procedures are performed in reverse order for the traditional construction of difference schemes; averaging of the transport equations occurs first and then the difference approximation of the obtained equations is constructed. The schemes constructed in such a manner can be treated as one of the classes of schemes using artificial viscosity. However, this viscosity is obtained not by phenomenonlogical means, as is customary, but is consistent with the form of the initial difference approximation of the Boltzmann equation. These schemes possess simplicity and good stability, meanwhile accuring high accuracy of the analysis. One of the characteristic features of the artificial dissipation constructed is that it turns out to be small in the boundary layer domain as compared with the true gas dissipation. The KCDS thereby organically realize the passage from modelling the inviscid part of the flow to modelling those domains where taking account of the viscosity and heat conduction is essential. Precisely this indeed permits utilization of the constructed apparatus to model a broad circle of problems studied least that are associated with the investigation of viscous separation flows, aswell as with the analysis of the heat transfer proceeding for such processes. The complexity of the solution of such problems is, to a significant degree, in the effective combination of the computation of processes occurring in both the viscous and inviscid parts of the flow.

A characteristic example of such flows is the flow around a step located in the stream. In this paper results are presented of an analysis of such a flow and their comparison with the data of full-scale experiments.

M. V. Keldysh Institute of Applied Mathematics, Academy of Sciences of the USSR, Moscow.
Translated from Inzhenreno-Fizicheskii Zhurnal, Vol. 58, No. 4, pp. 675-681, April, 1990. Original article submitted February 14, 1989.

0022-0841/90/5804-0519$12.50

1. METHODOLOGY OF THE NUMERICAL SOLUTION AND FORMULATION OF THE PROBLEM

A KCDS with corrections written for a plane two-dimensional flow [4] is used for the numerical solution:

$$\rho_t + (\rho u)^\circ_x + (\rho v)^\circ_y = \left[\frac{h^x}{c}(\rho u^2 + p)_{\bar{x}}\right]_x + \left[\frac{h^y}{c}(\rho v^2 + p)_{\bar{y}}\right]_y, \tag{1}$$

$$(\rho u)_t + (\rho u^2 + p)^\circ_x + (\rho u v)^\circ_y = \left[\frac{h^x}{c}(\rho u^3 + 3pu)_{\bar{x}}\right]_x + \left[\frac{h^y}{c}(\rho u v^2)_{\bar{y}}\right]_y +$$

$$+ \frac{M_\infty}{Re_\infty}\left[\frac{4}{3}(\mu u_{\bar{x}})_x + (\mu u_{\bar{y}})_y + (\mu v^\circ_x)^\circ_y - \frac{2}{3}(\mu v^\circ_y)^\circ_x\right], \tag{2}$$

$$(\rho v)_t + (\rho u v)^\circ_x + (\rho v^2 + p)^\circ_y = \left[\frac{h^x}{c}(\rho v u^2)_{\bar{x}}\right]_x + \left[\frac{h^y}{c}(\rho v^3 + 3pv)_{\bar{y}}\right]_y +$$

$$+ \frac{M_\infty}{Re_\infty}\left[(\mu v_{\bar{x}})_x + \frac{4}{3}(\mu v_{\bar{y}})_y + (\mu u^\circ_y)^\circ_x - \frac{2}{3}(\mu u^\circ_x)^\circ_y\right], \tag{3}$$

$$E_t + (u(E+p))^\circ_x + (v(E+p))^\circ_y = \left[\frac{h^x}{c}\left(u^2\left(E + \frac{5}{2}p\right)\right)_{\bar{x}}\right]_x +$$

$$+ \left[\frac{h^y}{c}\left(v^2\left(E + \frac{5}{2}p\right)\right)_{\bar{y}}\right]_y + \left(\frac{h^x}{c}\frac{1}{\rho(\gamma-1)}p^2_{\bar{x}}\right)_x +$$

$$+ \left(\frac{h^y}{c}\frac{1}{\rho(\gamma-1)}p^2_{\bar{y}}\right)_y + \frac{M_\infty}{Re_\infty}\left[\Phi + \frac{\gamma}{Pr}((\mu\varepsilon_{\bar{x}})_x + (\mu\varepsilon_{\bar{y}})_y)\right], \tag{4}$$

$$c = \sqrt{\gamma(\gamma-1)\varepsilon}, \quad E = \rho\frac{u^2+v^2}{2} + \rho\varepsilon.$$

The dissipative function has the form [5, p. 38]

$$\Phi = \frac{\partial}{\partial x}(\tau_{xx}u + \tau_{xy}v) + \frac{\partial}{\partial y}(\tau_{xy}u + \tau_{yy}v). \tag{5}$$

The system (1)-(4) is closed by the equation of state

$$p = \rho(\gamma-1)\varepsilon. \tag{6}$$

The sutherland law in the form

$$\frac{\mu}{\mu_\infty} = \left(\frac{\varepsilon}{\varepsilon_\infty}\right)^\omega, \quad 1/2 \leqslant \omega \leqslant 1. \tag{7}$$

is used in the problem. The system of difference euations (1)-(4) was made dimensionless in the ordinary manner

$$x = \tilde{x}h, \; u = c_\infty\tilde{u}, \; \rho = \rho_\infty\tilde{\rho}, \; v = c_\infty\tilde{v}, \; p = \rho_\infty c^2_\infty\tilde{p}, \; \mu = \mu_\infty\tilde{\mu}. \tag{8}$$

The difference scheme is supplemented by boundary conditions of the following kind the condition of stream drift is posed on the free boundaries, and the adhesion and non-penetratin conditions for the velocity and isothermy for ε on the solid walls

$$u = v = 0, \; \varepsilon = \varepsilon_w, \tag{9}$$

TABLE 1. Comparison of Computational and Experimental [7] Base Pressure Data

Modification number	δ/h	Re_∞	Experiment	Computation	
				grid 61×33	grid 90×50
1	1,25	$9{,}46\cdot10^3$	0,76	0,73	—
2	0,85	$1{,}48\cdot10^4$	0,72	0,68	0,69
3	0,725	$2{,}47\cdot10^4$	0,70	0,64	—
4	0,65	$3{,}19\cdot10^4$	0,50	0,66	—

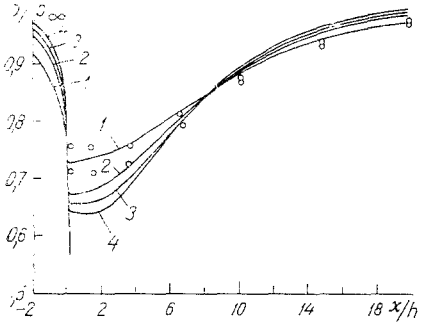

Fig. 1

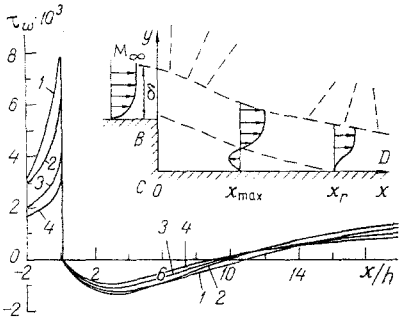

Fig. 2

Fig. 1. Pressure distribution p/p_∞ along the x axis for modifications 1-4 (numbers on the curves); points are experiment data [7] for modifications Nos. 1 and 2.

Fig. 2. Friction distribution along the x axis for modifications 1-4.

as well as the additional condition [3] assuring equality of the density of the stream to zero through the wall, which is realized in this case in the form $\partial p/\partial n = 0$ and is associated with the presence of the second spatial derivatives in the continuity equation (1).

Let us examine the conditions at the entrance boundary in greater detail. Given here are the laminar boundary layer parameters for a given thickness δ

$$\frac{u}{u_\infty} = \frac{14}{9}\frac{y}{\delta} - \frac{7}{9}\left(\frac{y}{\delta}\right)^4 + \frac{2}{9}\left(\frac{y}{\delta}\right)^7,$$

$$v = 0,\ p = p_\infty,$$

$$\frac{\varepsilon}{\varepsilon_\infty} = 1 + \sqrt{\mathrm{Pr}}\,\frac{\gamma-1}{2}\,M_\infty^2\left[1 - \left(\frac{u}{u_\infty}\right)^2\right] + \frac{\varepsilon_w - \varepsilon_e}{\varepsilon_\infty}\left(1 - \frac{u}{u_\infty}\right),$$

where $\varepsilon_e = \varepsilon_\infty\left(1 + \sqrt{\mathrm{Pr}}\,\frac{\gamma-1}{2}\,M_\infty^2\right)$ is the equilibrium internal gas energy at the wall.

Boundary conditions of a special kind that permit taking account of the influence of rarefaction waves being propagated upstream in the boundary layer are posed at subsonic points of the entrance boundary.

Parameters of the entrance boundary were given as initial conditions in the whole computational domain. In conformity with the dimensionless notation (8), $u_\infty = M_\infty$, $\rho_\infty = 1$, $p_\infty = (\gamma(\Gamma - 1))^{-1}$.

2. RESULTS OF THE NUMERICAL MODELLING

The characteristic example of a viscous supersonic flow is the flow around a step located in the stream. Despite its outward simplicity, this problem included many basis features inherent to the modelling of steady viscous separation flows, and can be considered as a serious calculation test.

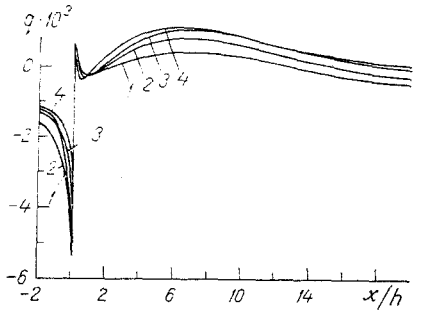

Fig. 3

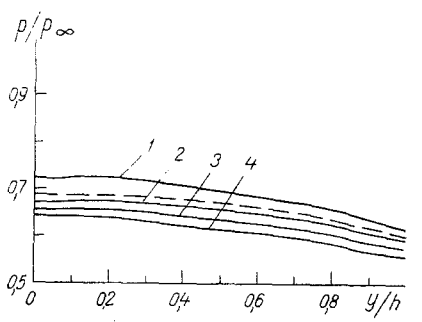

Fig. 4

Fig. 3. Heat flux distribution along the x axis for modifications 1-4.

Fig. 4. Base pressure distribution for modifications Nos 1-4; the dashed curve is a computation on a 90 × 50 grid for modification No. 2.

Experimental and theoretical results of investigations of problems of this kind are elucidated, in particular, in the monograph [6, Vol. 3, p. 18]. Experimental data on the laminar separation behind a step are presented in [7], and an analysis of laminar flow by using difference schemes for the Navier–Stokes equations with a compact approximation of third order accuracy in the smooth flow domain in [8].

A series of computations was performed by means of the KCDS for $M_\infty = 2.9$, and the Reynolds numbers and boundary layer thicknesses presented in the table,* which corresponds to the parameters of full-scale experiments [7]. The solid wall temperature was considered constant and was determined by the stagnation energy ε_0. In the Sutherland law (7) $\omega = 1$, $Pr = 0.72$, $\gamma = 1.4$. A spatial grid of 61 × 33 nodes condensing to the step boundaries is used in the computations, and a modification No. 2 was computed on a 90 × 50 node grid to check the accuracy.

For all four modifications the general flow pattern is close to that presented in [4]. A typical pattern of boundary layer interaction with an external ideal flow is realized here [6, Vol. 3, p. 48]: the supersonic compressible gas stream is separated from the step, passes through a rarefaction wave and is closed by a compression wave. Dependences of the pressure p/p_∞, friction $\tau_w = \mu\partial u/\partial n$, and heat flux $q = \lambda\partial T/\partial n$ along the horizontal (Figs. 1-3) and vertical (Fig. 4) surfaces of the specimen are presented in Figs. 1-4 for the modifications Nos. 1-4. All the flow characteristics, the heat flux, base pressure, magnitude of the friction, as well as the position of the separation point and attachment point of the stream vary monotonically in the selected range of parameters as the number Re_∞ changes.

The pressure distribution in front of the base corresponds to the data in [6, Vol. 3, p. 250] and reflects upstream propagation of the influence of the rarefaction wave that occurs as the flow turns to a distance $Re^{-1/2}$ (see Fig. 1). Reduction of the domain of influence with the growth of the number Re is seen. The pressure distribution behind the step (Fig. 1) has the following character: directly behind the step the pressure is approximately constant. The pressure increases with distance from the step in the main flow direction and has a maximal gradient to the left of the point of boundary layer attachment. Their the pressure gradient drops and the pressure is equalized. As Re_∞ changes from $9.5\cdot10^3$ to $3.\cdot10^4$ the value of x/h for which pressure equalization occurs behind the compression shock, diminishes from 22 to 15. This regularity is observed in both the numerical and the full-scale experiment [7]. The good agreement between the data of the full-scale experiment and the results of the computations is seen in Fig. 1.

A comparison between the experimental [7] and numerical values of the base pressure is presented in the table for different Reynolds numbers. As Re_∞ increases from $9.5\cdot10^3$ to $3.2\cdot10^4$ the base pressure drops by changing from the value $p' = p/p_\infty = 0.76$ to 0.50. The pressure obtained when using the Chapman theory [6, Vol. 2, p. 214] for the laminar mixing zone behind the step for zero boundary layer thickness ahead of the separation point is $p'_{ch} = 0.38$. The base pressure evaluated in this manner is independent of the Reynolds number. For comparison we present the value of the base pressure computed according to the Korst

*The Reynolds number is computed according to the step height h and the free-stream parameters.

theory [6, Vol. 2, p. 47] for a turbulent mixing layer: $p'_K = 0.18$. The good agreement between the results of the numerical and the full-scale experiments is seen for the first three modifications where laminar flow is observed. The difference does not exceed 6%, which is close to the accuracy of the full-scale experiment [7]. The base pressure drop as the Reynolds number increases indicates the existence of a transition flow mode behind the step. In the transition mode where flow turbulization is manifest, the agreement becomes worse (modification No. 4) since the problem formulation under consideration is oriented toward laminar flow analysis.

The location of the stream attachment point is seen well on the graph of the distribution of τ_w (Fig. 2). The separation point is always located below the edge of the step. The nature of the flow in the near-wall domain is traced clearly from the behavior of the friction and heat flux in Figs. 2 and 3. The gas accelerates in front of the step and cools off, then passes through the rarefaction wave and is again heated to a temperature close to T_0 below the point of return flow attachment. Additional heating of the gas because of stagnation of the return flow is observed in the neighborhood of the corner point C. The gas is heated in the whole return flow zone near the wall CD as compared with the flow up to the step and cools off behind the tail compression wave (Fig. 3). The Nusselt number distribution within the limits of the separation zone and outside it has a maximum whose position x_{max} relative to the point of stream attachment x_r is, according to [9], related as follows: $x_{max} < x_r$. In computations $x_{max} = (0.6 - 0.7)x_r$ is obtained. In this problem the boundary layer thickness before separation is close to the height of the step, consequently, viscous effects play a substantial role here and result in additional heating of the gas. This heating is due both to heat transport from the wall because of heat conduction and to transfer of the total enthalpy H from the mixing zone into the return flow domain ($H_{min} = 640$ in the mixing zone for modification No. 4, and $H_{max} = 8.27$ and $H_0 = 6.71$ in the stream separation domain). The effects mentioned result in $T > T_0$ in the return flow stagnation domains (here $q_w \sim Re_\infty^{-1}$).

The pressure and friction distributions [8] obtained for laminar flow around a step are qualitatively close to the data for modification No. 1 for $M_\infty = 3$, $Re_\infty = 3 \cdot 10^3$, $\delta = h$, $T_w/T_\infty = 2.8$.

The modification No. 2 was computed additionally on a 90 × 50 grid to confirm the accuracy (see the dashed curve in Fig. 4). The magnitude of the base pressure and its distribution along CD became closer to experiment data (see Table 1). The point of attachment was shifted downstream somewhat ($x_r = 12$). The relationship between its position and the Nusselt number maximum was conserved. The separation point was shifted closer to the corner of the step (from 0.12 to 0.07) and the maximal value of friction increased at the endface wall. The remaining flow parameters, including the heat fluxes, varied insignificantly.

Let us examine briefly the methodology of the experiment [7], with whose data the numerical results are compared. An annular profiled nozzle with a central body was used in [7], the total pressure in the receiver varied between 0.025 and 0.3 MPa. The model itself, which is a cylindrical body with an axisymmetric step whose surface is parallel to the flow axis is the central body. The model diameter ahead of the step is $d = 2r_1 = 20$ mm, and the step depth is $h = 2$ mm. Sampling the static pressure ahead of and after the step along its surface was carried out by using a tube of inner diameter $d_1 = 0.8$ mm. The Reynolds number was computed according to the free-stream parameters ahead of the step and the length of the central body between the nozzle critical section and the base exit. The research was performed in cold air ($T_0 = 280$ K) so that the temperature factor is $T_w/T_0 \simeq 1$. Manometers filled with a fluid with low specific gravity and low vapor elasticity (dibutylphthalate, specific gravity 1.041 g/cm^3, vapor elasticity 10^{-6} mm Hg) were used to measure the static pressure that was $2.5 \cdot 10^{-4}$ MPa. The initial vacuum pump evacuated the manometer and the tank cavities to a 10^{-6} mm Hg pressure during preparation of the experiments. The error in base pressure measurement was 2-4%. Determination of the Mach number at the nozzle exit was performed by the nucleus of the total pressure profile. The nonsymmetricity of the p/p_∞ profile within the limits of the nucleus (y = 2-12 mm) was $\Delta(p/p_\infty) \simeq 7\%$, which corresponds to a change in the Mach number M ~ 1%. The boundary layer thickness before separation was measured by using a total pressure tube (a microhood), the boundary of the annular stream and boundary layer nucleus was determined here. The approximate estimates performed on the influence of the parameter $\delta/r_1 \sim 0.2$ on the boundary layer characteristics on the convex axisymmetric surfaces showed that the boundary layer ahead of separation is close to planar in the case under consideration. This permits carrying out numerical modelling of this problem is a planar two-dimensional geometry.

Therefore, it is shown in the paper that the KCDS permit successful modelling of separation flows in supersonic streams of a viscous heat conductive gas.

NOTATION

$\bar{u} = (u, v)$ is the velocity; ρ is the density; p is the pressure; E is the total energy; ε is the internal energy; T is the temperature; Φ is the dissipative function; τ_{xx}, τ_{xy}, τ_{yy} are viscous stress tensor components; c is the sound speed; γ is the adiabatic index; μ, λ are the viscosity and heat conduction coefficients; Pr is the Prandtl number; Re is the Reynolds number; M is the Mach number; h is the step height; h^x, h^y are steps of the spatial grid; ω is the exponent in the Sutherland law; τ_w is friction; q is the heat flux; δ is the boundary layer thickness; n is the external normal to the surface; H is the total enthalpy. The subscripts w refers to the wall parameters, ∞ to the unperturbed stream, and 0 to stagnation.

LITERATURE CITED

1. T. G. Elizarova and B. N. Chetverushkin, Dokl. Akad. Nauk SSSR, 279, No. 1, 80-89 (1984).
2. T. G. Elizarova, Zh. Vychisl. Mat. Mat. Fiz., 27, No. 11, 1753-1757 (1987).
3. T. G. Elizarova and B. N. Chetverushkin, Zh. Vychisl. Mat. Mat. Fiz., 28, No. 5, 695-710 (1988).
4. A. N. Antonov, A. E. Duisekulov, and T. G. Elizarova, On Certain Results of Solving the Problem of Supersonic Viscous Flow Around a Backward Step Obtained on the Basis of Kinetically Consistent Difference Schemes. Preprint No. 165 Inst. Prikl. Mat. im. M. V. Keldysh Akad. Nauk SSSR, Moscow (1988).
5. L. G. Loitsyanskii, Mechanics of Fluids and Gases [in Russian], Moscow (1973).
6. P. Chen. Separation Flows, Three Volumes [Russian translation], Moscow (1972-1973).
7. A. N. Antonov, Prikl. Mekha. Tekh. Fiz., No. 3, 56-63 (1980).
8. A. D. Savel'ev and A. I. Tolstykh, Zh. Vychisl. Mat. Mat. Fiz., 27, No. 11, 1709-1724 (1987).
9. E. M. Sparrow and S. S. Kang, Int. J. Heat Mass Transfer, 30, 1237-1245 (1987).

METHOD OF NUMERICAL SOLUTION OF ONE-DIMENSIONAL MULTIFRONT STEFAN PROBLEMS

R. I. Medvedskii and Yu. A. Sigunov

UDC 536.42:519.6

A finite-element method with explicit isolation of fronts is proposed for Stefan problems with an arbitrary number of phase transition boundaries.

In conformity with practical requirement for the mathematical modelling of phase transitions it is necessary to perform explicit separation of the moving boundaries in the majority of cases, that not every numerical method permits doing. For instance, algorithms based on an enthalpy formulation [1, 2] or "blurring of the front" [3] that satisfactorily determine the temperature field, yield only a rough estimate of the phase front location. Numerous literature, for which a brief survey is contained in [4, 5], say is devoted to methods with explicit separation of fronts. Recently, several different modifications of application of the finite element method with deformable computational grids has been proposed in the direction of developing this approach for the solution of problems in domains with nonstationary boundaries [6-8]. The common disadvantage of both these and other finite-element methods proposed earlier is that different numerical schemes describe heat transmission within a single-phase domain and the front motion law, where the order of accuracy of the second schemes (in direct proximity of the front) is lower, as a rule, then for the first. Besides the degradation of the accuracy, the heterogeneity of the computation schemes results in complication of the algorithm for the solution, that grows strongly as the number of fronts increases.

Western Siberian Scientific-Research Geological Prospecting Petroleum Institute, Tyumen'.

Inzhenerno-Fizicheskii Zhurnal, Vol. 58, No. 4, pp. 681-689, April, 1990. Original article submitted January 30, 1989.

0022-0841/90/5804-0524$12.50